

Simulation of coating profile under plasma spraying conditions

Hurevich V, Gusarov A, Smurov I, Saint Etienne / France

Abstract. One of the key aspects of particle behaviour in the plasma jet is a stochastic nature of the injection process. Particles, which are characterized by size distribution, are injected into the plasma jet within a certain range of initial velocities. The velocity and size distribution determine the shape of the coating and the melting fraction. The aim of the present work is to study the influence of the spraying initial parameters on the main particle characteristics such as temperature, velocity, melt degree etc. at its impact to the surface. The one-dimensional heat-conduction equation involving phase transformations is solved numerically under the assumption of a particle spherical shape employing coordinate-transformation. Melting, evaporation and solidification interfaces are tracked continuously. The particle dynamic problem is solved as well. An integral criterion for coating modelling is obtained. All the above models are integrated into a self-consistent program complex.

1. Introduction

Plasma spraying represents a high-performance process of surface modification. It allows to produce coating layers on the surface of metals and alloys, which resist to corrosion, wear, fatigue, and other forms of surface degradation [1,2]. Thermal spraying has a wide range of application and offers possibility to make the coatings from relatively thin films and up to macroscopic structures.

A schematic overview of a thermal spray process is illustrated in fig.1. The particle is injected in the plasma jet with a carrier gas having diameter and velocity distribution. The injection of the particle is characterized by initial temperature and position of injection. After its injection, the particle are heated and accelerated by plasma jet. Particle

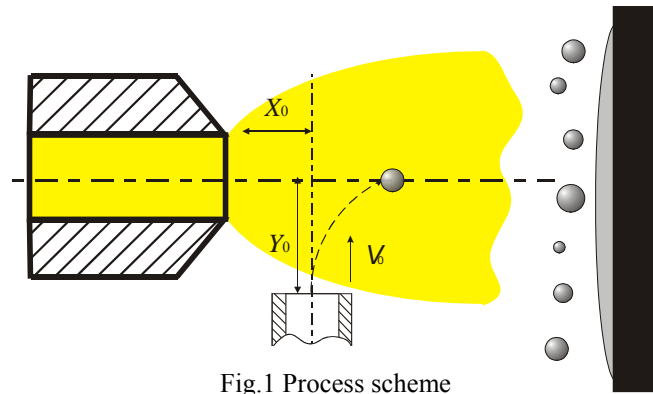


Fig.1 Process scheme

flying is characterized by duration of $10^{-2} - 10^{-4}$ s for typical particle sizes, considerable temperature gradients in the particle at the beginning of the flaying (between $0.5 \cdot 10^6$ K/m for metals and $50 \cdot 10^6$ K/m for ceramics). On this stage several problems take place. The first one is to solve transient non-linear heat conduction equation taking into account melting and solidification. The properties of the particle material can change during the heating because of a wide range of temperature. Therefore numerical integration of the heat conduction equation is carried out with allowance for thermal conductivity and specific heat capacity as

functions of the temperature. The second one is to take into account the evaporation law that can strongly influence convective particle heating

2. Mathematical model

The modelling of particle heating and acceleration in the plasma jet involves the following conjugated problems: particle dynamic heating, melting and evaporation. The particle is assumed to have a spherical shape. The mathematical model uses temperature and velocity fields, calculated or measured for an unloaded plasma jet. Therefore we neglect the particle influence on the plasma jet parameters.

2.1 Dynamic problem

Following forces affect a particle flying in a plasma jet: thermophoresis force, Magnus's force, drag force and gravity force. In the present work only gravity and drag forces are taken into account because thermophoresis and Magnus's forces are negligible compared to these ones [1]. In this case the dynamic equation for the particle can be written as follows:

$$\frac{d\vec{V}_p}{dt} = \frac{3}{4} \cdot C_D \cdot \frac{\rho_g (\vec{V}_g - \vec{V}_p) \cdot |\vec{V}_g - \vec{V}_p|}{\rho_p d_p} + \vec{g} \quad (1)$$

where \vec{V}_p is the particle velocity, \vec{g} is the gravity acceleration, \vec{V}_g is the gas velocity, ρ_p is the particle mass density, d_p is the particle diameter, C_D is the drag coefficient. The gravity acceleration is parallel-oriented Y-axis. The function $\vec{V}_g(X, Y)$ is assumed to be known (it may be taken from experimental measurements or calculations of unloaded plasma jet). The problem of C_D calculation is well studied in a number of works [5,6,9,10]. The expression for C_D calculation depends on the Reynolds number and is given as follows:

$$\begin{aligned}
C_D &= \frac{24}{\text{Re}} & \text{Re} < 0.2 \\
C_D &= \frac{24}{\text{Re}}(1 + 0.187 \text{Re}) & 0.2 < \text{Re} < 2.0 \\
C_D &= \frac{24}{\text{Re}}(1 + 0.11 \text{Re}^{0.81}) & 2.0 < \text{Re} < 21.0 \\
C_D &= \frac{24}{\text{Re}}(1 + 0.189 \text{Re}^{0.62}) & 21.0 < \text{Re} < 500.0
\end{aligned} \tag{2}$$

where $\text{Re} = \frac{\rho_g |\vec{V}_g - \vec{V}_p| d_p}{\mu_g}$ is the Reynolds number; μ_g is

the dynamic viscosity of the plasma forming gas. The first equation is based on the Stocks solution for the flow around a sphere under assumption of a small Re; the second equation is based on the Oseen approximation; the third and fourth ones are based on the experimental data by Beard and Pruppacher [6]. Equations (1) and (2) may be solved numerically by a fourth order Runge-Kutta method.

2.2 Particle-gas energy transfer

There are two ways of heat transfer from the plasma to the particle surface: by radiation and by convection. Convection can be represented as follows:

$$Q_c = \text{Nu} \cdot \lambda_g \cdot \frac{T_g - T_{ps}}{\pi d_p}, \tag{3}$$

where Nu is the Nusselt number; λ_g is the gas thermal conductivity; T_{ps} is the particle surface temperature; $T_g(X, Y)$ is the ambient gas temperature. The function is considered to be known like $\vec{V}_g(X, Y)$ in equation (1). There are several approximations of the Nusselt number in different Re ranges:

$$\text{Nu} = 2 + 0.6 \text{Re}^{0.5} \text{Pr}^{0.33}; \quad \text{Re} < 2 \tag{4}$$

$$\text{Nu} = 1.05 \text{Re}^{0.5} \text{Pr}^{0.3}; \quad 2 < \text{Re} < 500 \tag{5}$$

where Pr is the Prandtl number. Equation (4) is the well-known Ranz-Marshall expression. Equation (5) is an experimental approximation for turbulent flow condition discussed in detail in [4, 10].

The expression for calculating the radiation flux is written down assuming that the radiation energy flux acts directly to the particle surface (transparency is neglected). In this case, the radiation energy flux is:

$$Q_r = \sigma_B \varepsilon_p (T_g^4 - T_{ps}^4) \tag{6}$$

where ε_p is the normalized emissivity factor; σ_B is the Stefan-Boltzmann constant. The total energy flux, which represents the sum of the convective and radiation ones:

$$Q = Q_r + Q_c \tag{7}$$

2.3 Heat conduction problem

There are two general ways to solve the heat conduction equation with phase transformations. The first method is based on the enthalpy formulation approach for the solution of the phase change problem [11]. The interface position

does not appear explicitly in the calculation. The enthalpy function is used to account for phase change. The main advantage of this method is simplicity. It is possible to determine the interface position within the accuracy of one calculation cell. It corresponds to the first accuracy degree only.

The second method, which is applied in the present work, is based on explicit definition of the interfaces positions [14]. This method is more precise, but it requires interfaces tracking. Several phase combinations take place during particle heating in the plasma jet that is followed by cooling: solid, solid-liquid (with melting and evaporation interfaces), liquid (evaporation interface), solid-liquid-solid (melting and resolidification interfaces), liquid-solid (resolidification interface). Each phase state requires its own mathematical problem definition and solution. In the present work only the general solid-liquid case is described in details. Equations for solid-liquid case can be written as follows:

$$\frac{\rho_p \partial h(T_1)}{\partial t} = \frac{1}{r^2} \frac{\partial}{\partial r} (r^2 \lambda_1(T_1) \frac{\partial T_1}{\partial r}), \quad r \in (0; \gamma) \tag{8}$$

$$\frac{\rho_p \partial h(T_2)}{\partial t} = \frac{1}{r^2} \frac{\partial}{\partial r} (r^2 \lambda_2(T_2) \frac{\partial T_2}{\partial r}), \quad r \in (\gamma; \xi) \tag{9}$$

$$T_1(\gamma, t) = T_2(\gamma, t) = T_m \tag{10}$$

$$\rho L_m \frac{d\gamma}{dt} = \lambda_1(T_m) \frac{\partial T_1}{\partial r} \Big|_{r=\gamma+0} - \lambda_2(T_m) \frac{\partial T_2}{\partial r} \Big|_{r=\gamma-0} \tag{11}$$

$$\rho L_v \frac{d\xi}{dt} = \lambda_2(T_2) \frac{\partial T_2}{\partial r} + Q(T_2), \quad r = \xi \tag{12}$$

$$\frac{dT_s}{dt} = f(T_s) \tag{13}$$

$$\frac{\partial T_1}{\partial r} = 0, \quad r = 0 \tag{14}$$

$$\begin{aligned}
T_1(r, t_{SLstart}) &= T_{init}, & r &\in [0; \gamma]; \\
T_2(r, t_{SLstart}) &= T_m, & r &\in [\gamma; \xi]
\end{aligned} \tag{15}$$

where t is the time; r is the radius; $T_1(r, t)$, $T_2(r, t)$ are the temperature distributions in the solid and the liquid phase, respectively; L_m is the latent heat of melting; L_v is the latent heat of evaporation; T_s is the particle surface temperature; T_m is the melting point; $h(T)$ is the specific enthalpy of the particle material; $\lambda_1(T)$, $\lambda_2(T)$ are the known thermal conductivities for the solid and liquid phase, respectively; $t_{SLstart}$ is the initial time of solid-liquid scheme calculation; T_{init} is the initial temperature distribution in the particle. The problem is characterised by the two mobile bounds: evaporation interface $\xi(t)$ and solid-liquid interface $\gamma(t)$. These bounds divide the calculation domain into two parts $[0; \gamma]$ and $[\gamma; \xi]$, respectively. Expressions (8) and (9) are the heat conduction equations in solid and liquid phases written in spherical geometry (the particle is assumed to have a spherical shape). The temperature at the solid-liquid interface is always constant and equal to T_m (10). Equation (11) represents the Stefan boundary condition at the solid-liquid interface. Equation (12) is the

boundary condition at the particle surface, which involves energy flux Q through the surface of the particle (7). Equation (13) represents an evaporation rate depending on the particle surface temperature. Condition (14) ensues from the particle symmetry. Expressions (15) represent the initial conditions for equations (9)-(10).

2.4 Evaporation law

Particle evaporation influences particle heating and melting. Moreover, particle diameter decrease due to evaporation causes trajectory changing and influences particle acceleration. In the present work the model of rapid surface evaporation with backpressure has been implemented. The model is based on conservation of mass, momentum and energy through a thin Knudsen layer [12]. Knight shows that in this case jump condition for the Knudsen layer can be written as follows:

$$\left\{ \begin{aligned} \frac{P}{P_s} &= \sqrt{\frac{T}{T_s}} \left[(\beta^2 + 0.5) e^{\beta^2} \operatorname{erfc}(\beta) - \frac{\beta}{\sqrt{\pi}} \right] + \\ &+ \frac{1}{2} \left(1 - \sqrt{\pi} \beta e^{\beta^2} \operatorname{erfc}(\beta) \right) \\ \frac{T}{T_s} &= \left[\sqrt{1 + \pi \left(\frac{\gamma - 1}{\gamma + 1} \frac{\beta}{2} \right)^2} - \sqrt{\pi} \frac{\gamma - 1}{\gamma + 1} \frac{\beta}{2} \right]^2 \end{aligned} \right. \quad (16)$$

where γ is the ratio of specific heats ($\gamma = 5/3$ for monatomic gases); P is the gas pressure; P_s is the saturated vapour pressure (it can be measured or calculated by Clausius-Clapeyron equation[13]); β is the dimensionless velocity of vaporisation $M = u/\sqrt{\gamma RT} = \beta\sqrt{2/\gamma}$; M is the Mach number; u is the local flow velocity outside the Knudsen layer. Equation (16) is adequate only if the flow outside the Knudsen layer is subsonic. The Mach number can not be greater than 1.

For the spherical particle, the radius decreases due to evaporation that can be written as:

$$\frac{dr_p}{dt} = \sqrt{\frac{2R}{T}} \frac{\beta P \mu}{\rho_p k}, \quad M \leq 1; \quad (17)$$

where T and β are taken from the solution of (16); ρ_p is the mass density of the particle material; μ is the molecular mass of the particle.

2.5 Coating profile

To simulate coating profile obtained by the plasma spraying technique a detailed study of the initial condition of the particles injection is required. Stochastic behavior of particle entry defines coating thickness and its profile. The particles have two distributed variables: initial particle diameter and initial injection velocity (r_p and V_0 , respectively). These two parameters cause particles trajectory distribution. If the V_0 and r_p were constant, the particles would have the same trajectory. The first variable

depends on the way of particle fabrication and in the present work it is accepted the Gauss's distribution for it. The initial velocity depends on the way of the particles entering to the plasma jet, and will be considered in details below. There is an extra factor, which determines the profile of the coating. This is a non-stationary behavior of velocities field. This factor is not taken into account in the present work.

In reality, the particles are introduced into the plasma jet through an injector pipe by a particle-carrier gas. Velocity and density distributions at the outlet are determined by the injector pipe configuration. In the developed model we assume that the initial particle velocity distribution is equal to the gas velocity distribution and the particle mass flow at the outlet is constant. The above assumptions correspond to long injector pipes, where the particles have time to reach stationary mode. Long injector pipes are used in most of industrial plasma torches [1,2].

Gas flow at the outlet obeys the parabolic Poiseuille law [3]. Therefore we can assume that particle velocity is distributed according to the Poiseuille law as well.

The thickness of the coating, obtained by plasma spraying technology, depends on spraying time, powder flow rate, etc. For real application purposes it is sufficient to obtain a function, which is in proportion to coating thickness distribution on the substrate without having its absolute quantity, e.g. coating profile.

There is a set of particle trajectories lying in the same plane α , which is perpendicular to the substrate plane (see fig 2). The plane α forms a straight line at intersection with the substrate plane. To deposit a coating on the substrate, a nozzle moves along X-axis, like it is shown in fig.2. For this case coating thickness distribution will be uniform along X-axis. Therefore calculating coating thickness distribution only along Y-axis is required.

Calculating particle trajectories within a range of

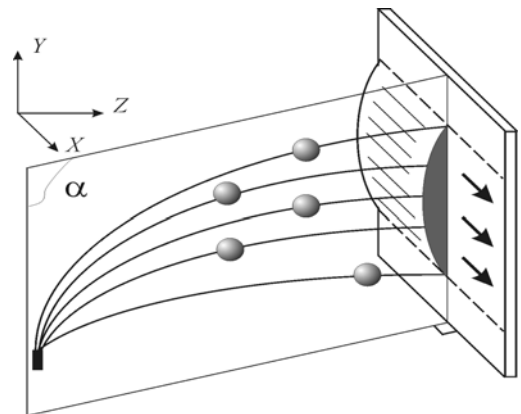


Fig.2 Particle flying scheme

initial velocities and with an initial particle radius makes it possible to obtain the mesh function $Y_p = G(V_0, r_p)$, where Y_p is the coordinate of the impact with the substrate.

Based on the above assumptions and distribution laws, the expression for coating profiles calculating is obtained:

$$h = \int_0^{V_{max}} \frac{V_0^3}{dy} (V_0, Y_p) V_0 e^{-\frac{(r_0(V_0, Y_p) - \bar{r})^2}{2\sigma^2}} dr_0 dV_0, \quad (18)$$

where \bar{r}_0 is the mean radius; σ is the standard deviation of the Gauss's distribution. The same technique was used to obtain melting and evaporation fraction distributions.

3. Results and discussion

The simulation results of Al_2O_3 spraying are shown in figures 3,4. Temperature and velocity distribution of unloaded plasma jet are taken from [6]. All the other input data are given in Table 1.

The influence of diameter (left column) and velocity (right column) dispersions on a single particle heating and dynamics is shown in fig. 3. Deviation of the trajectory from the X-axis is determined by the radial velocity component of the ambient gas and the initial particle velocity, which is usually oriented along the Y-axis. The radial velocity component always is abaxial. The trajectory for the particles with greater diameter and, consequently, with greater inertia is determined essentially by initial velocity. The influence of the inertia for the smaller ones is much less, therefore in this case the radial velocity component of the ambient gas is a decisive factor (see fig. 3.a, see fig. 3.b).

The velocity of the particle decreases with radius decreasing (see fig. 3c) because its mass is proportional to the third power of the particle diameter, and the drag force is proportional to the square power only. For the particles with the different initial velocities and the same size (see fig. 3d) the particle velocity is determined by the velocity of the ambient gas. To better understand particle behaviour for the case at hand considering trajectories is required (fig. 3b). As a rule, the velocity of ambient gas decreases with the distance increasing from the jet axis. Therefore the trajectories with higher deviations from the jet axis correspond to smaller particle velocities.

In the present work only the influence of the injection velocity and the particle size dispersion were analysed. Two major factors directly influence the particle heating: particle trajectory and particle diameter. The particle temperature decreases along with the diameter because the particle mass is proportional to the third power of the particle diameter, and the surface area and the energy flux are proportional to the square power only. On the other hand a greater particle diameter causes a smaller velocity and a longer flight-time. Moreover, the particle diameter determines the particle trajectory and, consequently, the ambient gas temperature and energy flux to the surface of the particle. A strong dependence of the above mentioned parameters on the particle diameter is analysed in fig. 3. A general tendency revealed in our calculations showed up the particle temperature decreasing with the radius increasing. The second factor, e.g. particle trajectory, depends on the initial velocity and the particle diameter. The trajectories with a greater deviation from the jet axis correspond to smaller particle temperatures (see fig. 3f, fig.3b).

The temperature in the centre of the particle (see fig. 3g, fig. 3h) depends on thermophysical properties of the particle material and the temperature at the surface of the particle.

Calculations carried out for different flight-times showed up considerable temperature gradients at the beginning of the particle heating and their practical absence at the impact to the substrate.

Coating profiles for radius dispersion of 4 μ m (uninterrupted line) and 6 μ m (dashed line) are shown in fig.4a. The profiles have Gaussian distribution shape and they are in qualitative agreement with experimental results, which is shown in Fig.4.c. [Technical report of INODCOT project].

The powder with a wider size distribution gives a wider coating profile but only in a certain extend. The main limiting factor for the coating width is the plasma jet geometry, mainly its diameter because the flying off particles cannot take part in coating formation.

A wider diameter distribution causes smoothing of the maxima. This tendency can be observed not only for the coating profile, but also for the entire distributed parameters (see fig.4.b).

Coating profile has a fringe, which is obtained during the simulation and can be observed in the experimental results as well. The radial velocity component of the plasma velocity distribution influences the light particle fraction and, probably, causes this fringe.

The evaporation fraction distribution has two marked maxima that correspond to two competitive factors. The first one is caused by a light fraction which is deposited lower (see fig.3a). The second one is caused by the long duration of the flying and corresponds to the heavier particles.

The melt fraction distribution (see fig.3.d) shows that the particles are well melted.

Acknowledge

The present research was supported by the Directorate General for Science Research and development of European Commission under BRITE Euram Project INODCOT BE-5040.

Table 1. Conditions for the simulation

Plasma forming gas	Ar
Particle material	Al_2O_3
Initial particle velocity	15 m/s (for fig.3 only)
Initial particle temperature	300 K
Particle injection position	$X_0=0$; $Y_0=-2$ mm (relatively plasma nozzle, see fig.1)

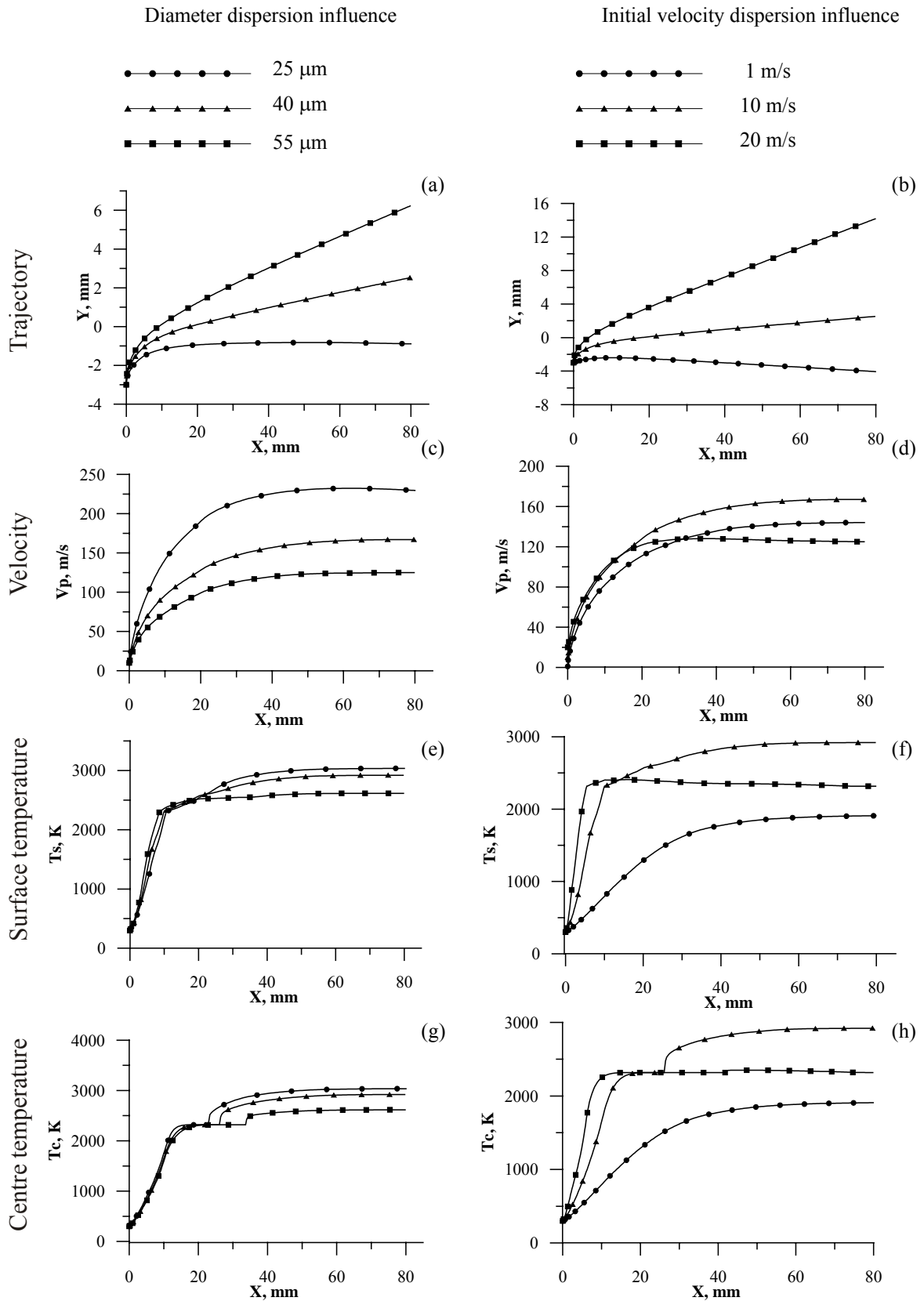


Fig. 3. Single particle behaviour along the plasma jet (distance X is counted from the plasma nozzle): trajectory $Y=f(X)$; velocity $V_p = f(X)$; particle surface temperature $T_s = f(X)$; particle centre temperature $T_c = f(X)$

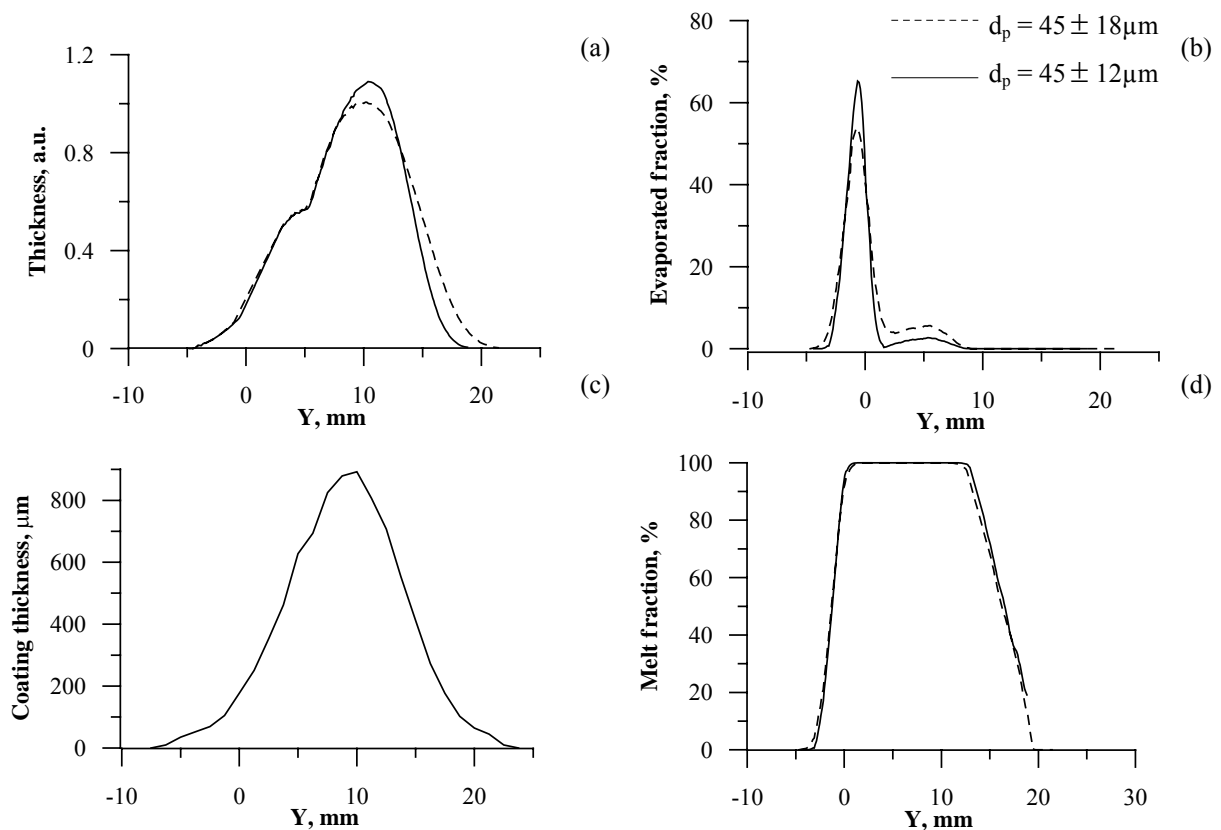


Fig. 4. Coating profile : (a) simulation, (c) experiment (8 consecutive passages of plasma torch along X-axis). Distributions of the coating melted (d) - and vapour fractions (b) at the substrate. Orientation of X,Y-axes is shown in Fig. 2

REFERENCES

- Ladru F., Lugscheider E., Landes K. Reusch A. Untersuchungen zum Zusammenhang von Plasma-, Partikel- und Schichteigenschaften mittels optikel Messverfahren. Endbericht zur AIF 9622: RWTH Aachen, 1996. 130p.
- Plasma processes in Electronics Production/ In 3 Vol. / A. Dostanko, S. Kundas, S. Bordusov, A. Ilyuschenko, E. Lugscheider. Minsk: FUAinform, 2000.
- Poiseuille J., Recherches expérimentelles sur le mouvement des liquides dans les tubes de très petits diamètres. Comptes Rendus 11, 961-967, 1041-1048 (1840).
- Deposition of plasma coating // V.V.Kudinov, P.Yu.Pekshev, V.E.Belaschenko et al. Moscow: Nauka, 1990. – 406 p. (in Russian).
- Reynolds O., An experimental investigation of the circumstances which determine whether the motion of water shall be direct or sinuous, and of the law of resistance in parallel channels. Phil. Trans. Roy. Soc. 174, 935-982 (1883).
- Vardelle V, Vardelle A.Fauchais P., Boulos M. Plasma – Particle Momentum and Heat Transfer: Modelling and Measurements /AICHE Journal, Vol.29, No.2, 1983.-Pp. 236-242
- Yang Y. Coddet C. Imbert M. Numerical modeling and simulation of particle behaviours in an HVOF International Thermal Spray Conference, 25-29 May 1998, Nice, France, 1998.- P. 431-438
- Burov I.S. To calculation of heat transfer of material dispensed particles with plasma / Physic and Chime of Material Treatment, 1979.- №4.-c.43-48
- Kudinov V.V. Plasma Coating.- Moscow: Nauka, 1977. – 184 p. (in Russian).
- Chen X. Particle heating in a thermal plasma / Proc. of VIII Intern. symp. on plasma chem. Tokyo, 1987.- Vol.1.- Pp.4-12
- D.A. Knoll, D.B. Kothe, and B. Lally: A new nonlinear solution method for phase-change problems/ Numerical Heat Transfer, Part B, 35:439-459/1999 /Copyright © 1999 Taylor & Francis. p 439-459.
- Charles J. Knight/ Theoretical Modeling of Rapid Surface Vaporization with back pressure/ AIAA Journal Vol.17, No 5, May 1979/ p. 519-523
- A. Gusarov and I Smurov/ Target-vapour interaction and atomic collision in pulsed laser ablation/ Appl Phys. 34 (2001) p.1147-1156.
- Modelling of thermo-physical processes of impulse laser influence on metals / A.A.Uglov, I.Yu.Smurov, A.M.Lashin, A.G.Guskov. – Moscow: Nauka, 1991.– 228 p. (in Russian).